© S. Hirzel Verlag
Stuttgart

Impulse Response Measurement of Individual Ear Canals and Impedances at the Eardrum in Man

M. Joswig
Lehrstuhl für allgemeine Elektrotechnik und Akustik, Ruhr-Universität Bochum

Impulse Response Measurement of Individual Ear Canals and Impedances at the Eardrum in Man

Summary

The impulse response measurement is a simple method to determine in one step (I) the individual cross-sectional area function of human ear canals and (II) the plane-wave termination impedance at the eardrum for a frequency range of 1–20 kHz.

Firstly we give the theoretical and numerical solution for the "inverse problem" of calculating an arbitrary area function from its impulse response. To examine this method in practice some test measurements were performed with custom-made brass tubes which yield excellent results. Also the impedance values match well to the horn impedance which could be calculated analytically.

Individual results from the measurement of humans are reported for 8 subjects. When their impedances were transformed to a common reference plane by means of the actual area functions, the deviations between individual subjects were significantly reduced compared to the constant-tube assumption. The reference plane of the chosen termination impedance is 5 mm in front of the ear canal end quite near the beginning of the inclined eardrum. The achieved results are in agreement with anatomical data and published values of the eardrum impedance.

Messung der Impulsantwort individueller Gehörgänge und Trommelfellimpedanzen beim Menschen

Zusammenfassung

Die Messung der Impulsantwort ist eine einfache Methode zur gleichzeitigen Bestimmung (I) der individuellen Querschnittsfunktion des menschlichen Gehörgangs und (II) der Abschlußimpedanz an der Stelle des Trommelfells in einem Frequenzbereich von 1–20 kHz.

Zuerst wird die theoretische und numerische Lösung für das inverse Problem der Berechnung einer beliebigen Querschnittsfunktion aus der Impulsantwort angegeben. Zur praktischen Überprüfung dieser Methode wurden einige Versuchsmessungen an spezialangefertigten Messingrohren ausgeführt, welche hervorragende Ergebnisse liefern. Auch stimmen die Impedanzwerte gut mit der Horn-Impedanz überein, die analytisch berechnet wurde.

Des weiteren wird über Einzelergebnisse der Messung am Menschen für acht Personen berichtet. Wenn deren Eingangsimpedanzen mit Hilfe der tatsächlichen Flächenfunktionen in eine gemeinsame Referenzebene transformiert wurden, konnten die Abweichungen zwischen individuellen Ergebnissen stark vermindert werden verglichen mit der Annahme eines Rohres konstanten Querschnitts. Die Referenzebene für die gewählte Abschlußimpedanz liegt 5 mm vor dem Gehörgang und in der Nähe des Anfangs des geneigten Trommelfells. Die erzielten Ergebnisse stimmen mit anatomischen Daten und Literaturwerten der Trommelfellimpedanz überein.

Mesure de la réponse impulsionnelle du conduit auditif et de l'impédance au tympan chez l'homme

Sommaire

La mesure de la réponse impulsionnelle est une technique simple pour déterminer à la fois (I) le profil individuel de section du conduit auditif et (II) l'impédance en onde plane à l'emplacement du tympan pour une bande de fréquences allant de 1 à 20 kHz.

Tout d'abord nous donnons la solution théorique et numérique du «problème inverse» qui consiste à déterminer un profil de section arbitraire à partir de la réponse impulsionnelle. Pour tester la validité de la méthode, nous avons procédé à des mesures sur des tuyaux de cuivre construits à cet effet; les résultats sont excellents. Les valeurs d'impédance coïncident bien aussi avec celles d'un pavillon, que l'on peut déterminer analytiquement.

Des mesures sur oreilles humaines ont été faites avec le concours de huit sujets. Lorsque l'on ramène leurs impédances d'entrée à un plan de référence commun en utilisant le profil de section réel, la dispersion interindividuelle se trouve sensiblement réduite par comparaison avec les calculs effectués en supposant le conduit de section constante. Le plan de référence choisi est à 5 mm du fond auditif, tout près du bord externe du tympan. Les résultats obtenus sont en accord avec les données anatomiques et les valeurs publiées d'impédance du tympan.

Received 2 January 1992,
accepted 7 July 1992.

Manfred Joswig, Lehrstuhl für allgemeine Elektrotechnik und Akustik, Ruhr-Universität Bochum, Postfach 10 21 48, D-4630 Bochum 1, now at Lehrstuhl für Meßtechnik, RWTH Aachen, Templergraben 55, D-5100 Aachen.

1. Introduction

While extensive data of impedance measurements exist for the eardrum in the low frequency range, only limited and contradictory data are available above 4 kHz [1–4]. Obviously, high frequency measurements demand more sophisticated test equipment and some theoretical investigations on the effects of acoustic wave propagation. The low frequency approximations of the ear canal – lumped acoustical element or uniform tube – do not hold when the wavelengths become comparable to the geometrical dimensions. For the $\lambda/4$ criterion, the equivalent frequency would be 12 kHz but a severe degradation in measurement reliability must be expected down to a few kHz. The problem may be minimized in experiments with animals by cutting the ear canal short to realize a microphone position just in front of the eardrum. However, for the in vivo measurements of humans this method cannot be applied and thus we must determine the impact of ear canals on the impedance determinations on an individual base.

This treatment can be achieved by knowing both the impedance at some reference point and the ear canal area function of individual ears [5]. When we neglect the spatial extent of the eardrum and its vibration in eigenmodes by abstracting to the plane-wave solution, the theory is exact. Unfortunately, Hudde's experimental solutions turned out to be very sensitive to the shape of the cross-sectional area functions, only the straighter ear canals were resolved sufficiently. The early insight into these limitations motivated the development of a concurrent method for ear canal determination [6]. After some initial and encouraging results the approach was complemented by an impedance calculation. Now it forms a complete procedure for the in vivo determination of human "eardrum impedances" up to 20 kHz – or strictly speaking for the determination of plane-wave termination impedances at the beginning of the inclined human eardrum.

2. The algorithm

The principle idea of determining an area function from purely acoustical measurements is evident: Suppose, a tube of varying diameter is approximated by a number of tube slices. The cross-sectional area function is piecewise constant with discrete steps at the junction of two slices. Each step will reflect portions of the incoming wave. In case of a spike each reflection appears as a little spike also (see Fig. 1). The location of the sought area step is related to the impulse delay, while the signal amplitude determines the amount of

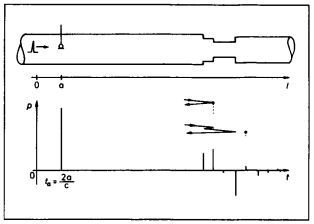

Fig. 1. The principle idea for determining the area function by impulse response: Each step at the border of two tube slices will produce a reflection. Its amplitude describes the amount of change and its arrival time the place of change. The superposition by multiple reflections will inhibit a direct solution for more than one area step, instead it demands the solution of an "inverse problem".

area change. However, this principle situation is complicated by multiple reflections. Although of smaller magnitude, they increasingly contaminate the direct reflections at later times. So the exact determination of cross-sectional area functions demands the solution of an "inverse problem".

These inverse problems are well known in all parts of physics and consequently several solutions exist for, e.g., geophysical exploration or remote sensing. To our knowledge, the most elegant solution was proposed for an acoustical problem and given by Sondhi and Gopinath [7]. Their goal was to measure the changes in cross-sectional area function of human vocal tracts during vocalization. The derived solution is analytical, so it does not demand the approximation of a stepwise constant area function. Adapted to our problem, the relevant results are summarized below.

Given a tube with volume $V(x)$ from $x = 0$ to $x = a$, the univocal solution for $V(x)$ can be derived from (notice: $\varrho = c = 1$)

$$V(a) = \int_0^a f(a,t)\,dt \tag{1}$$

with an auxiliary function $f(a,t)$ which is defined by the Fredholm integral equation of

$$f(a,t) + \frac{1}{2}\int_{-a}^{a} h_Z(|t-\tau|)\,f(a,\tau)\,d\tau = 1 \quad |t| \leqq a. \tag{2}$$

The impulse response $h_Z(t)$ is determined from the convolution integral of the unit-volume velocity impulse $u(t)$ and the reflected pressure response $p(t)$ by

$$p(t) = \int_0^t h_Z(t-\tau)\,u(\tau)\,d\tau. \tag{3}$$

To calculate the volume $V(x)$ at $x = a$, $h_Z(t)$ must be known by measurement in the interval $0 \leqq t \leqq 2a$. The sought area function $A(x)$ follows by differentiation of eq. (1).

Obviously, the impulse response $h_Z(t)$ is the time-transformed input impedance $Z(x)$ at $x = 0$. While well defined in theory, the impulse response which is more related to the actual measurements of sound pressure levels by a microphone is given by

$$\hat{h}_p(t) = \delta(t) + h_p(t), \tag{4}$$

derived from

$$p_T(t) = \int_0^t \hat{h}_p(t-\tau)\, p_W(\tau)\, d\tau \tag{5}$$

with $p_W(t)$ as the incoming source signal and $p_T(t)$ corresponding to the measured microphone voltage.

To utilize $h_p(t)$ the necessary modifications of eq. (2) were proposed in [6, 8]; the most general proof, however, is given by Sondhi & Resnick [9] in the relation

$$2\, h_p(t) = h_Z(t) - \int_0^t h_Z(\tau)\, h_p(t-\tau)\, d\tau \tag{6}$$

which substitutes eqs. (1), (2) by

$$V(a) = \int_0^{2a} f(a,t)\, dt - a \tag{7}$$

and

$$f(a,t) + \int_{-t}^{0} h_p(t+\tau)\, f(a, 2a+\tau)\, d\tau = 1 \quad 0 \leqq t \leqq 2a. \tag{8}$$

The numerical solution of eq. (8) is efficiently performed by the Levinson-algorithm which is applicable to the whole class of Toeplitz-matrices, see e.g. [10]. In Fig. 2, we sketch the final matrices for solving eqs. (8), (7) as used for this study.

While now the solution of the inverse problem is simple, determining the impulse response $h_p(t)$ imposes additional difficulties. The deconvolution by eq. (5) is "ill posed", minimal perturbations cause severe numerical instabilities. To overcome these problems, a modification of Tikhonov's regularization procedure [11] was used by calculating

$$\hat{h}_p = (P_W^T \cdot P_W + \alpha E)^{-1} \cdot P_W^T \cdot p_T, \tag{9}$$

where P_W is the Toeplitz-matrix of the source signal p_W, E is the unit matrix, and the upper index T denotes transposed matrices. The optimum for the regularization factor α depends on the actual signal to noise ratios.

Once the area function of a tube is known, the calculation of the termination impedances at any plane from the given impulse response is straight forward. Measuring two known termination standards, e.g., hard wall and infinite tube, yields the source signal $p_0(t)$ and the source impedance $Z_1(\omega)$. Any third determination of $p_T(t)$ is sufficient to obtain the input impedance $Z_E(\omega)$ at the microphone. This result can be transformed by means of chain matrices or lattice filters (see Fig. 3).

nslice = 1

$$\begin{bmatrix} 1 & h_1 \\ h_1 & 1 \end{bmatrix} * \begin{bmatrix} f_1 \\ f_2 \end{bmatrix} = \begin{bmatrix} 1 \\ 1 \end{bmatrix}$$

$$vol_1 = 2 * f_1$$
$$area_1 = vol_1 - 1$$

nslice = 2

$$\begin{bmatrix} 1 & 0 & h_1 & h_2 \\ 0 & 1 & 0 & h_1 \\ h_1 & 0 & 1 & 0 \\ h_2 & h_1 & 0 & 1 \end{bmatrix} * \begin{bmatrix} f_1 \\ f_2 \\ f_1 \\ f_2 \end{bmatrix} = \begin{bmatrix} 1 \\ 1 \\ 1 \\ 1 \end{bmatrix}$$

$$vol_2 = 2 * (f_1 + f_2)$$
$$area_2 = vol_2 - (vol_1 + 1)$$

nslice = 3

$$\begin{bmatrix} 1 & 0 & 0 & h_1 & h_2 & h_3 \\ 0 & 1 & 0 & 0 & h_1 & h_2 \\ 0 & 0 & 1 & 0 & 0 & h_1 \\ h_1 & 0 & 0 & 1 & 0 & 0 \\ h_2 & h_1 & 0 & 0 & 1 & 0 \\ h_3 & h_2 & h_1 & 0 & 0 & 1 \end{bmatrix} * \begin{bmatrix} f_3 \\ f_2 \\ f_1 \\ f_1 \\ f_2 \\ f_3 \end{bmatrix} = \begin{bmatrix} 1 \\ 1 \\ 1 \\ 1 \\ 1 \\ 1 \end{bmatrix}$$

$$vol_3 = 2 * (f_1 + f_2 + f_3)$$
$$area_3 = vol_3 - (vol_2 + 1)$$

nslice = 4

.....
.....

Fig. 2. The algorithm for area determination by eqs. (7) and (8): The solution can utilize the Toeplitz structure of the matrix and is performed most efficiently by a modified Levinson recursion.

Our actual measurements were evaluated up to 20 kHz for the impedance calculation and up to 60 kHz for the area functions. To maintain precise results in this frequency range the effect of losses cannot be neglected as was done in the preceding formula. The necessary corrections should, however, preserve the simplicity of the algorithm to yield an overall simple approach. To reach this aim was easy for the impedance transformations, we just introduced the complex wavenumber

$$k\,[\mathrm{mm}^{-1}] = 1.8 \cdot 10^{-5} f\,[\mathrm{Hz}] - \mathrm{j}\, 7.5 \cdot 10^{-6} \sqrt{f\,[\mathrm{Hz}]} \tag{10}$$

to Fig. 3. The specific numerical values were derived for viscosity losses of a cylindrical tube with 4 mm radius neglecting dispersion effects [12a–13].

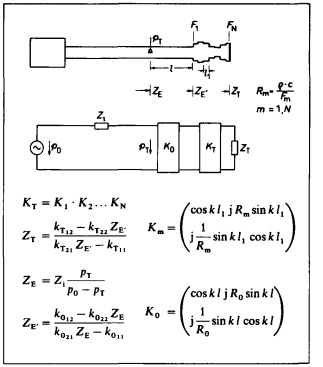

Fig. 3. Calculation of the impedance Z_T at the eardrum: The area function of the ear canal is approximated by small slices and determined by inversion of the impulse response. The transformation from Z_E at the microphone to any other termination plane is based on the product of chain matrices K_0 and K_T.

A comparably exact correlation for the area function in eqs. (7) to (9) must also depend on the square root of frequency. However, this correction would significantly complicate the time-based calculations. Instead we tried the most simple approach of frequency independent compensation. Given in dB/m, it will progressively increase the later reflections of $p_T(t)$ before the deconvolution is performed in eq. (9). We adjusted the attenuation factor to 2.6 dB/m empirically which compensated best in the fit of different area functions. To our surprise, this value can also be obtained as the solution of the exact, i.e., frequency dependent calculation of attenuation losses by eq. (10) for $f = 24$ kHz. The empirical choice turns out to be reasonable since 24 kHz is just the approximate spectral mean of the utilized impulse source by spark discharge.

3. Test results

In practice, the accuracy of deconvolution and impedance determination depends crucially on a well suited acoustic source. The main criteria are (I) the acoustic impulses must be reproducible to allow for averaging, i.e., S/N improvement, and a single calibration run to determine p_0 and Z_1, (II) the rise-time must be very short (50 µs) to yield a reasonably well-posed deconvolution by eq. (9), (III) the source spectrum should be flat for the frequency range of impedance measurements (100 Hz – 20 kHz), (IV) in the same range, the source impedance should be free of poles and zeros.

With respect to these requirements, a number of acoustic transducers were tested. We used dome tweeters from different manufacturers, an oscillating plasma column, a free running spark discharge utilizing an high voltage capacitor and finally its triggered version based on an ignition coil. The best impulse source, found at the date of the measurements, was the free running spark discharge with a repetition rate of approximately 3 sec. Although we had severe problems with source wavelet variations initially, they could be fixed by experiments with electrode form and material and, even more important, the instruction to avoid any near-electrode air motion for a whole test session. With these precautions, the acoustic advantages of the spark source were so evident that it was chosen in spite of the well known difficulties in safety and electrical interference.

Fig. 4 shows the final experimental arrangement. To avoid reflections from the source or the left tube end, the tube lengths were designed to be appropriate for time windowing the impulse response. The generation of standing waves between electrodes and microphone was reduced by inserting damping material in between. Above 23 kHz, some higher modes can propagate. Their impact was found to be most dependent on how the microphone was attached to the tube. Different insertion depths and microphones were tested, the best results were achieved with a condensator micro-

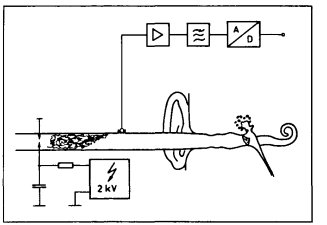

Fig. 4. Principle components of the measurement set-up: The sound source is a free running spark discharge with a repetition rate of approximately 3 sec. It triggers a transient recorder for the A/D-conversion. Between electrodes and microphone, the tube is filled by damping material.

phone of 3 mm diameter (B & K 4138) which was set flush to the tube wall.

In Fig. 5, the source wavelet is shown with a peak amplitude of 128 dB for 10 μsec and a total length of 200 μsec. The reflections are caused by the closed tube end and yield the source reflectance r_i at the microphone. The attenuation factor 2.6 dB/m of the previous chapter could be verified by the decay in reflected amplitudes.

To test the accuracy of the whole approach a set of 12 different brass tubes with precisely known area functions was constructed. In any session for one tube, 24 measurements were performed and the 16 most correlated source wavelets were averaged. The area function determined by this joint impulse response was in very good agreement to the corresponding brass tube's data for all geometries. The most critical case of a stepwise changing, unconcentric tube is shown in Fig. 6; the achieved result indeed justifies the neglection of higher modes in our calculations.

While testing area functions was simple, it was significantly more difficult to verify the accuracy of

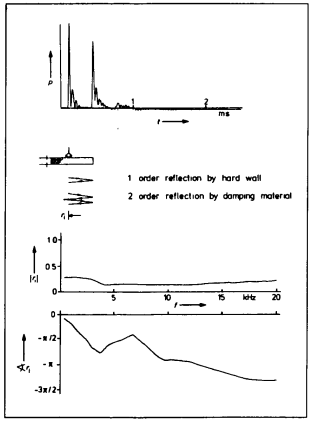

Fig. 5. Source signal and source reflectance: The source signal has a length of 200 μsec, its peak amplitude is 128 dB for 10 μsec. At later times, multiple reflections from the hard wall are visible which allow for calculation of the source reflectance r_i. Due to the damping material and the optimized microphone coupling, its values are very smooth.

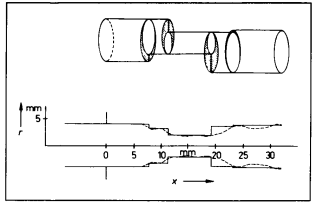

Fig. 6. Area determination for a brass tube: The unconcentric geometries are chosen to obtain an experimental estimate for the maximum influence of higher mode distortion. The delayed increase for the step at 19 mm shows the effective acoustic area function.

impedance determinations. These tests depend on known impedances with magnitudes similar to the expected eardrum impedance. From the few theoretical solutions that can be calculated analytically, the most appropriate one for our purposes was a conical horn in an infinite wall [12b, 14]. Instead of the throat impedance Z_{ha}, we chose a transform value Z_M to exclude possible higher mode distortions at the throat. Then once again theory and experimental results agreed very well (see Fig. 7).

Of course, the ultimate error estimate must rely on the combination of both approaches. We must experimentally determine a non-constant area function and calculate the transformed termination impedance on the basis of these data. The results of this scenario are shown in Fig. 8. In front of the acoustic load by the conical horn (the "eardrum") is a brass tube with its varying diameter (the "ear canal"). Indeed the accuracy of our results has decreased but still the obtained impedance shows sufficient similarity to the theoretical calculation. The common alternative to assume a straight tube as in some previous publications about eardrum impedance would depreciate all our results above 2 kHz.

The one problem not seen here but still left in our arrangement is the accuracy of impedance measurements at low frequencies. Our results are only reliable above 1 kHz, below this the short duration of the source impulse caused problems in cases of more rigid termination impedances like, e.g., the human eardrum.

4. The impedance at the eardrum

Given the excellent results for the test measurements, it was surprising enough to find great difficulties in the

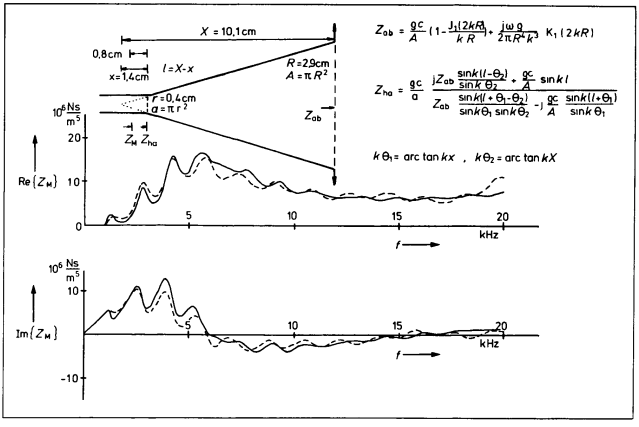

Fig. 7. Theoretical calculation and experimental determination for a non-trivial test impedance: The radiation impedance Z_{ab} of a massless piston in an infinite wall is given in [12b, 14]. The transformation to Z_{ha} at the plane of the horn throat is done by [12b]. The reference plane of the test impedance Z_M is 8 mm behind the throat to avoid higher mode distortions. —— computed, — — measured.

determination of in situ impedances at the human eardrum. The new problems were due to the effects of tube coupling to the ear canal. Seen analytically, we introduced an additional unknown without further information and thus cannot resolve its influence. The minimum requirements for the coupling were already described by Zwislocki [15] – keeping the measuring device steady relative to the head and obtaining a tight seal. For our measurements, his conclusions are proven again:

"Considering the difficulties arising from the anatomy of the ear, the theoretical precision of the acoustical method itself becomes of secondary importance".

In the course of our investigation, it took us several sessions with dozens of subjects to recognize all the unknowingly introduced problems. As a final aim, we wanted to reduce the effects of coupling to a pure change in area function which can be resolved by the presented theory. Fig. 9 shows, from back to forth, three sets of ear insert systems utilized in our measurements. Each set has cones with decreasing diameters to allow for best seal in the individual ear canal entrances. The two cone sets in front are connected to the measuring tube by brass adapters.

The first experiments were performed by means of the cone set in the back row of Fig. 9. The best fitting cone was screwed onto the measuring tube and then the whole unit was inserted into the ear canal. When analyzing the data in the following weeks, we found that in most cases the insert cone was facing the ear canal wall instead of the tympanic membrane. All these membranes were contaminated by hard wall reflections and thus the impedance determination yielded unreasonable results.

For the second session, we chose the black plastic inserts commonly used in otoscopes. They allowed for a clear visualization of ear canal and tympanic membrane. Once this position was reached, the measuring tube was connected without remove, shift or tilt of the insert. This time no hard wall reflections appeared but the results were dominated by strong resonances at 8 and 16 kHz. It turned out that they were caused by the air volume between the outer insert wall and the ear canal since the narrow end of the insert was too small.

The third attempt was undertaken with our custom made brass cones of larger end diameters. Additional-

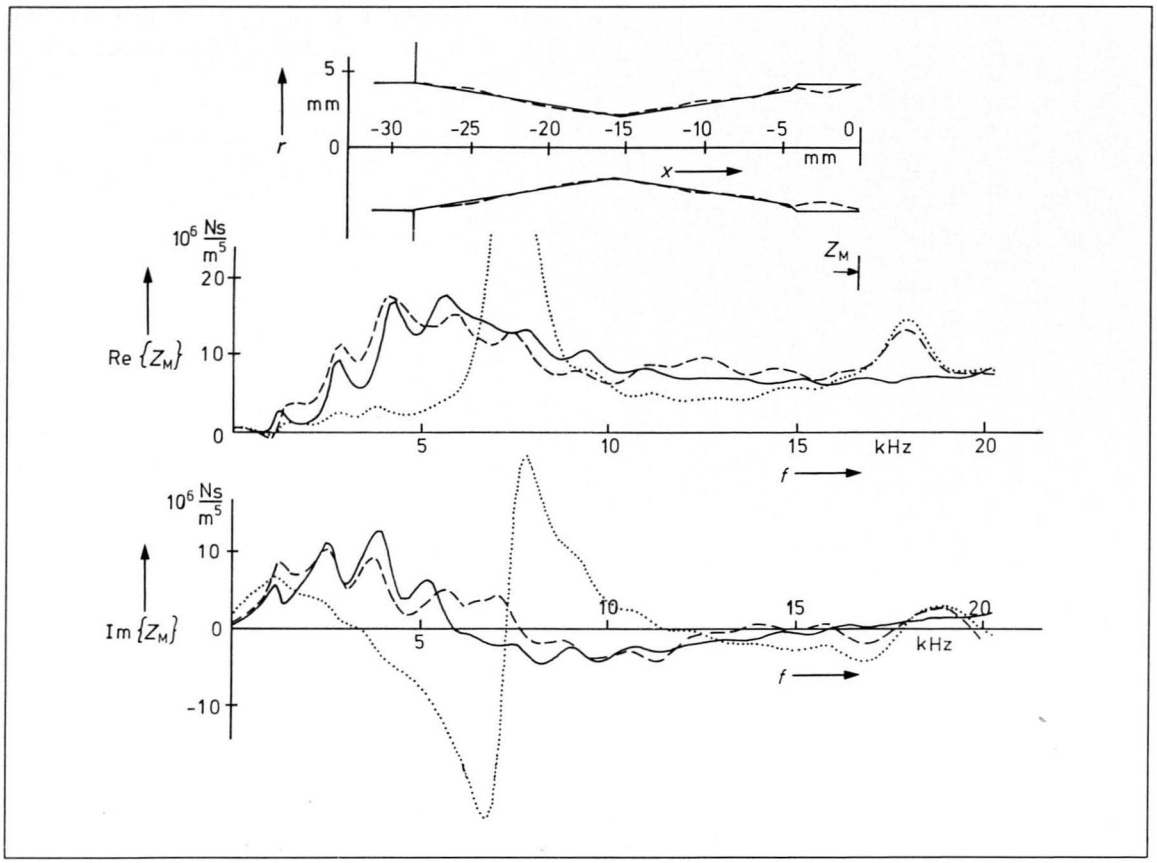

Fig. 8. The test impedance Z_M of Fig. 7 is connected via a narrowing to the measuring tube. Based on the experimental determination of the area function, the impedance transformation yields good results. The assumption of a constant tube diameter gives misleading values above 2 kHz. —— computed, —— measured, · · · · transformation with constant shape.

Fig. 9. Photo of different cone sets: Each row was used for a whole measuring session. The cones have decreasing end diameter from left to right. For the two sets in front, the additional cone adapters to the measuring tube are shown at right; the cones of the back row were screwed up directly.

ly, a little whole was drilled perpendicular to the cone axis to avoid any air shifting through the tube when sliding in the cone adapter. The ventilation hole is closed by the inserted tube at its final position but efficiently prevents any air motion that would otherwise destabilize the spark discharge.

The measurements start by visual inspection through the inserted cone and the subsequent tube attachment. Then some test measurements are performed to monitor the reflections at the junction of cone and ear canal. The corresponding signal amplitudes can be further minimized by slightly rotating the tube and pulling the pinna manually. Fig. 10 shows by a typical example which magnitude of these reflections remains. This residue may be caused by the sudden change in cross-sectional areas from circular cone to oval-shaped ear canal. Once the optimal adjustment is achieved, the subsequent procedure is as for the test measurements: 16 out of 24 signals are averaged to determine the area function and the termination impedance. The session was performed with 8 subjects

– 5 men and 3 women in the age of 20 to 35 years; all our reported results are achieved by this third attempt documented in Fig. 11 [16].

In order to compare any termination impedances of the human ear canal, they must be specified for a common reference plane. Planes that are defined by some fixed distance from the cone end are unreasonable because the insertion depths vary significantly between subjects. It would be possible to determine the individual distance to the tympanic membrane by manually inserting a stick; but this is a tedious and risky approach in routine sessions. Distances determined this way also show deviation because the point of contact depends on the lateral stick position relative to the eardrum's tilt. To our opinion, the best solution would be to adjust the reference plane by some properties of the measured impedance itself. Surprisingly enough, this is possible with the typical impulse response for our sessions shown in Fig. 10. There are two significant peaks, both of them arise from reflections in the zone of the eardrum. The first one does change in magnitude with each subject, the latter is always dominant and is about half as big as the source pulse. This second peak causes the rigid-wall behavior of the termination impedance for higher frequencies. The effect is very pronounced and constant for all subjects, it was firstly reported by Hudde [4]. He found impedance values at the eardrum which are above 10 kHz comparable to a hard wall termination. Utilizing this knowledge, we can derive a common reference plane for the transformed impedances to lie some millimeters in front of the cause for peak 2. According to our observations, this reflection is caused by the far end of the inclined tympanic membrane since mechanical distance controls yielded place short before peak 2 when a stick was inserted until eardrum contact was felt.

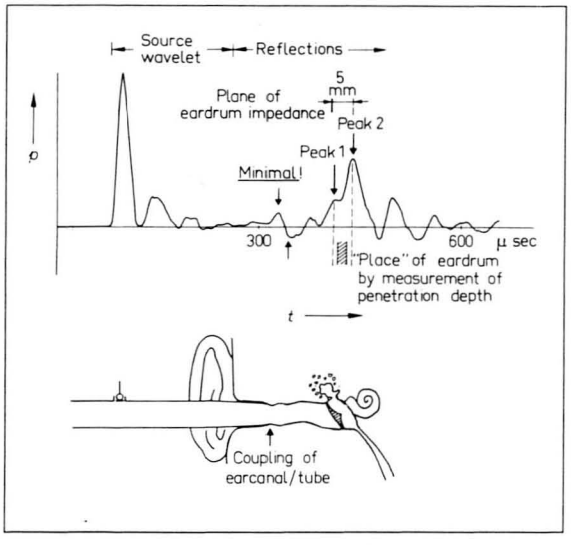

Fig. 10. Impulse response for an actual measurement of human ear canal and eardrum: The coupling between cone and ear canal must be adjusted to minimize the reflections at 350 μsec. When inserting a measuring stick manually, it indicates contact with the eardrum at a point which corresponds to a reflection between peak 1 and peak 2.

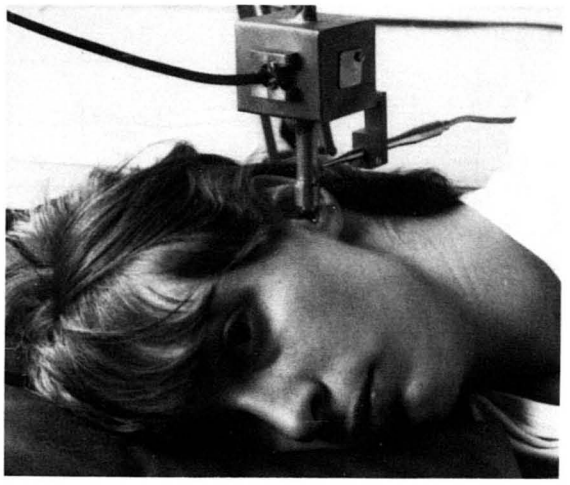

Fig. 11. Photo of the measuring tube: The spark discharge is located in the cubic brass box at top, a condensor microphone with preamplifier is attached below. The measuring tube continues for 75 cm at top of the box (not seen), its lower end is connected to the eardrum via a set of cones with different end diameters to fit best the individual size of ear canals.

To avoid possible misunderstandings it is necessary now to discuss in more detail what we mean by the term "impedance at the eardrum". The eardrum is inclined and does not interact with incoming waves at a single point. The sound energy is reflected not only by parts of the eardrum but as well as by the walls of the middle ear [17]. The eardrum itself vibrates in a variety of frequency dependent modes. So any point impedance determined physically at the eardrum would only express a very local behaviour. Instead, by our investigations we want to determine the effective acoustic behaviour of the eardrum for sound propagating in the ear canal. It is best characterized by the ratio of plane wave reflections to the incident wave at some median eardrum location, so the reflection coefficient $r(\omega)$ would be the appropriate parameter. If we assume locally constant geometry, any minor change in the reference plane of $r(\omega)$ would just affect the phase angle but not the absolute value and thus ease the comparisons. However, the eardrum reflectance is not a common parameter in literature, from all the papers about the eardrum behaviour it is only given in [4, 18–19]. So here we report both, the reflection coef-

ACUSTICA
Vol. 77 (1993)

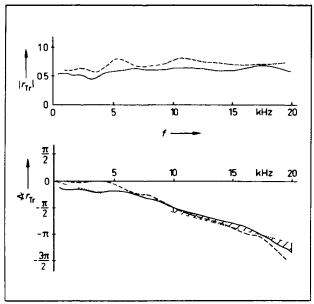

Fig. 12. Plane wave reflectance at the eardrum by different authors: Both results are based on a reference plane where the phase spectrum between 10 to 20 kHz is most similar to a fictitious plane 5 mm in front of an hard wall. —— Joswig, – – – Hudde (1983 b), · · · · 5 mm before rigid wall.

ficient and the associated plane wave termination impedance at the eardrum. The common reference plane for all our subjects is determined by matching the phase spectra to those of a fictitious place 5 mm in front of a hard wall. The similarity is determined by fitting least squares in the frequency range 10 to 20 kHz (Fig. 12), the transformations are performed every half millimeter. By this definition, our results are directly comparable to Hudde's calculations performed for the same reference plane.

All the transformations are based on the actually determined area functions of the ear canal. Fig. 13 shows the overlay of individual impedances and area functions. The effective ear canal lengths, i.e., the distances from cone end to reference plane vary from 12 to 21 mm and indicate the great differencies in penetration depths. To obtain an estimate for the systematic error that would otherwise be introduced by the assumption of an uniform ear canal, the transformations in Fig. 14 are performed on the same input impedances but with constant tube diameters. As already mentioned in the introduction, the results have significantly greater deviation above 4 kHz.

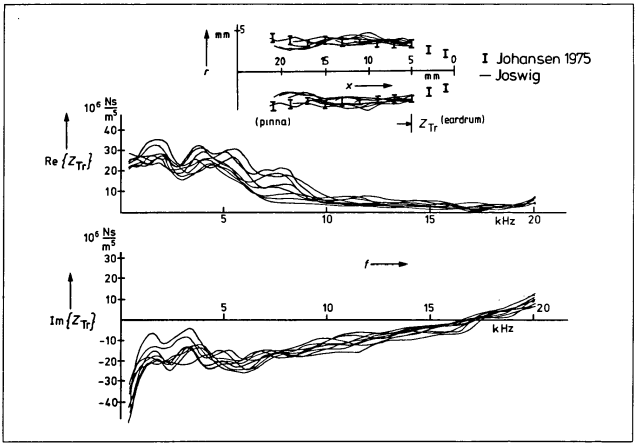

Fig. 13. Individual ear canal area functions and impedances at the eardrum for 8 subjects: The common reference plane is found by transforming the impedances every 0.5 mm and comparing the phase spectra (see Fig. 12). The area functions are in good agreement with [22] if a shift of 5 mm is applied also.

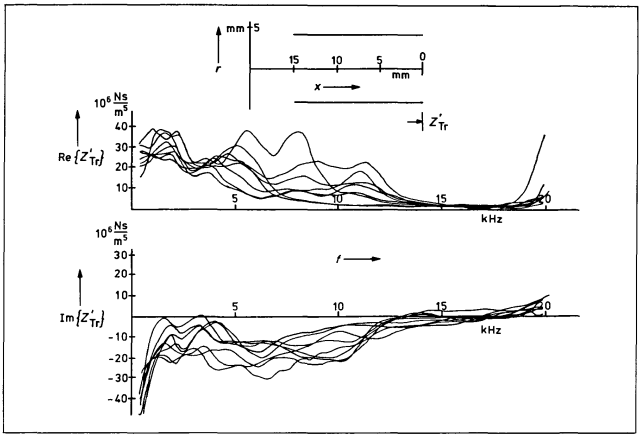

Fig. 14. Calculation of impedances at the eardrum for straight ear canals: Based on the same data as for Fig. 13, we assume a constant area function for the ear canal. The transformation will yield significantly larger deviations between the subjects.

Any further interpretation of our impedance results must be based on the eardrum's inclination. In sound propagation, the incident wave first reaches the outer part of the eardrum resulting in peak 1. The mass of the eardrum will dominate all reflections for higher frequencies, so the decreasing gap to the ear canal end will act as an acoustic horn. This smooth impedance matching excludes greater reflections; once the end of the gap is reached, the remaining energy is reflected in peak 2. So the deviations found experimentally in the time delay between the two peaks will indicate some different inclinations of the eardrum. The values derived from our data yield 4 to 7 mm for the effective lengths of wave propagation along the tympanic membrane and agree well with recent anatomical data [20–21]. With this interpretation, the reference plane for our termination impedance (5 mm in front of an hard wall) lies in the zone of the real eardrum, approximately at its beginning ("Top of Drum" of Fig. 1 in [21]).

In an earlier attempt, Johansen [22] measured the shape of the human ear canal. He determined its area function by taking a rubber cast to obtain the volume increment every 2 mm. In Fig. 13, we show his data converted to ear canal diameters with his standard deviations; our results fit very well if we once again assume that the reference plane is located 5 mm in front of the ear canal end. Another support for our data is [23] reporting an average distance of 16 mm between the tip of an ear mould and the contact to eardrums (13 subjects with a range of 11 mm to 19 mm). We can compare these data since penetration depths of even different couplings are primarily limited by the bony part of the ear canal. Assuming the distance between our reference plane (near "Top of Drum") and the point where a probe touches the eardrum to be 3 mm will fit both results quite well.

In Fig. 15 we compare published impedances at the eardrum with a frequency range above 2 kHz [1–4, 23]. The curves do not yield an overall agreement which is satisfactory, but impedances are strongly dependent on the chosen reference plane. Hudde's [4] plane is the same as ours, so similarities between both curves are reasonable. In general, the other authors did not report all necessary details and it is difficult to decide on the location of their reference planes. Some indirect hints exist, e.g., from the penetration depth we can conclude that Morton and Jones [23] determined their

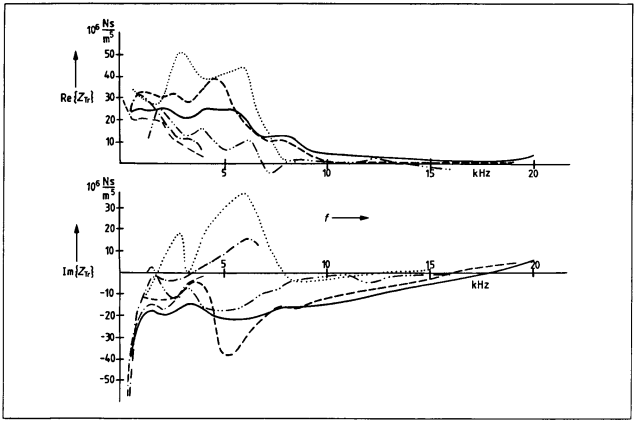

Fig. 15. Impedances at the eardrum by different authors: Except for our data, only the results of Hudde [4] are based on the individual determination of ear canals. Both impedances are defined for the same reference plane while the other authors do not describe this detail explicitly. —— Joswig, — — Hudde (1983 b), · · · · Mehrgardt, Mellert (1977), — · · — Blauert, Platte (1976), — · — Zwislocki (1970), — — · Morton, Jones (1956).

impedance in a plane 3 mm behind ours. Although there is no compelling evcidence, this may also be true for Zwislocki [1]. Fig. 16 displays his data derived from 22 subjects and our results. Their transformation 3 mm towards the middle ear gives excellent agreement in the reactance while resistance values still diverge above 3 kHz.

By our measurements it was not possible to resolve any effects caused by the acoustic reflex. To test its impact the reflex was elicited for three subjects contralateral by white noise of 100 dB SPL. The additional measurements were performed immediately after the normal impedance determination, neither tube nor insert were removed to ensure a precision of approximately 5% [24]. Nonetheless, no systematic change was observable in the data.

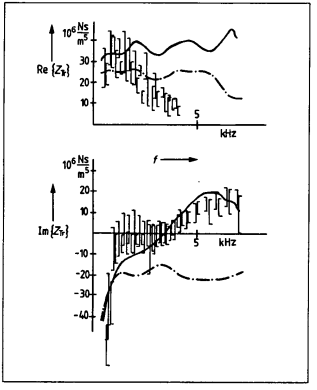

Fig. 16. The agreement with Zwislocki [1] is enhanced significantly if our data are transformed 3 mm towards the middle ear. This transformation is based on a constant tube with the specific wave resistance $R = 9.2 \times 10^6$ Nsm^{-5} as assumed in [1]. ——Joswig + 3 mm to middle ear, — · — Joswig, Zwislocki (1970)] 12 female, [10 male.

One explanation would be that the reflex was elicted all the time by the spark discharge pulse itself. All of our investigations were performed at the same amplitude level, so no statement is possible about amplitude dependencies. However, from other observations we can conclude that a permanent elicitation is not probable by the impulse itself. Firstly, the subjective sound impression was more that of a silent crack than a big bang because of the short duration. Secondly, the delay time of the acoustic reflex is at least 20 msec [25]. With a recording time of only 3 msec, any significant effects must be caused by the previous impulse. But the low repetition rate of about 3 sec would allow for the reflex to decay before the next measurement starts. So the nonresolution must more probably be contributed to the difficulties in determining rigid terminations for lower frequencies. As stated before, the spectral energy of the spark discharge source is not sufficient here. Explaining the effect this way is also consistent with other reports that found contributions of the acoustic reflex only below 1.5 kHz [3–4, 26–28].

5. Conclusions

The impulse response measurement is an elegant and reliable method to determine in vivo both the individual ear canal area function and the broadband termination impedance at place of the human eardrum. For the impedances, the reference plane can be defined by purely acoustic criteria without the need for mechanical adjustment. The impedance transformations based on the actual area functions reduce the inter-subject deviations significantly. The achieved results agree well with anatomical data of the ear canal and some published impedance curves if a common reference plane can be established.

The spark discharge impulse source limited the range of measurement to 1–20 kHz. Dome tweeters did resolve the lower frequencies in some prior test runs but their limited rise time excluded them from this study. However, this restriction must not concern the design of future equipment. (I) Tweeter technology has improved over the years and (II) some resolution of area functions can be sacrified once the principle knowledge about stable impedances above 10 kHz was derived. So we could compromise the determination of area functions to half the number of slices to defuse the ill-posed deconvolution process.

As a result, the more versatile tweeter sources could combine the determination of area functions and impedances above 1 kHz by impulse response with the steady state measurement of standing wave ratios to obtain reliable low frequency impedances. So the implementation into one unit could promise an universal and easy to use tool suited for the clinical diagnostics.

Acknowledgement

All theoretical investigations and experiments were performed at Lehrstuhl für allg. Elektrotechnik und Akustik of Ruhr-Universität Bochum. I wish to thank Prof. Blauert for his support and Dr. Hudde for the initial impetus to this work and for the many valuable discussions. Dr. Falkenstein assisted the measurements with humans, a grant by Geers-Foundation, FRG supported part of the equipment. After joining the Institut für Geophysik of RUB, Prof. Harjes enabled me to conclude the data interpretation. The initial manuscript received a very thorough review from Prof. Khanna.

References

[1] Zwislocki, J. J, An acoustic coupler for earphone calibration. Special report LSC-S-7 Syracuse Univ., Syracuse NY 1970.

[2] Blauert, J., Platte, H. J., Impulsmessung der menschlichen Trommelfell-Impedanz. Zeitschrift für Hörgeräte-Akustik **15** [1976], 34–44.

[3] Mehrgardt, S., Mellert, V., Transform characteristics of the external human ear. J. Acoust. Soc. Amer. **61** [1977], 1567–1576.

[4] Hudde, H., Measurement of the eardrum impedance of human ears. J. Acoust. Soc. Amer. **73** [1983 b], 242–247.

[5] Hudde, H., Estimation of the area function of human ear canals by sound pressure measurements. J. Acoust. Soc. Amer. **73** [1983 a], 24–31.

[6] Joswig, M., Hudde, H., Eine Meßrohrmethode zur Bestimmung der Querschnittsfunktion von Rohren. Fortschritte der Akustik – DAGA 1978, VDE-Verlag, Berlin 1978, 597–600.

[7] Sondhi, M. M., Gopinath, B., Determination of vocal-tract shape from impulse response at the lips. J. Acoust. Soc. Amer. **49** [1971], 1867–1873.

[8] Burridge, R., The Gelfand-Levitan, the Marchenko, and the Gopinath-Sondhi integral equations of inverse scattering theory, regarded in the context of inverse impulse-response problems. Wave Motion 2, North Holland publishing Co. 1980, 305–323.

[9] Sondhi, M. M., Resnick, J. R., The inverse problem for the vocal tract: Numerical methods, acoustical experiments and speech synthesis. J. Acoust. Soc. Amer. **73** [1983], 985–1002.

[10] Robinson, E. A., Treitel, S., Digital signal processing in Geophysics, in: Applications of digital signal processing, Oppenheim, A. V. (ed.), Prentice Hall, Englewood Cliffs NJ 1978, 474–479.

[11] Franklin, J. N., On Tikhonov's method for ill-posed problems. Math. Comp. **28** [1974], 889–907.

[12] Olson, H. F., Acoustical engineering. D. van Nostrand Co., Princeton NJ 1957, a: 113 ff, b: 90 ff.

[13] Meyer, E., Neumann, E. G., Physikalische und technische Akustik. Vieweg Verlag, Braunschweig 1975, 99 ff.
[14] Beranek, L. L., Acoustic measurement. John Wiley, New York 1949, 118 ff.
[15] Zwislocki, J. J., Some measurements of the impedance at the eardrum. J. Acoust. Soc. Amer. **29** [1957], 349–356.
[16] Joswig, M., Individuelle Ohrkanalbestimmung und Trommelfell-Impedanzmessung beim Menschen. Fortschritte der Akustik – DAGA 1984, DPG-Verlag, Bad Honnef 1984, 663–666.
[17] Rabbitt, R. D., A hierarchy of examples illustrating the acoustic coupling of the eardrum. J. Acoust. Soc. Amer. **87** [1990], 2566–2582.
[18] Lawton, B. W., Stinson, M. R., Standing wave patterns in the human ear canal used for estimation of acoustic energy reflectance at the eardrum. J. Acoust. Soc. Amer. **79** [1986], 1003–1009.
[19] Stinson, M. R., Revision of estimates of acoustic energy reflectance at the human eardrum. J. Acoust. Soc. Amer. **88** [1990], 1773–1778.
[20] Stinson, M. R., Lawton, B. W., Specification of the geometry of the human ear canal for the prediction of sound-pressure level distribution. J. Acoust. Soc. Amer. **85** [1989], 2492–2503.
[21] Chan, J. C. K., Geisler, C. D., Estimation of eardrum acoustic pressure and of ear canal length from remote points in the canal. J. Acoust. Soc. Amer. **87** [1990], 1237–1247.
[22] Johansen, P. A., Measurement of the human ear canal. Acustica **33** [1975], 349–351.
[23] Morton, J. Y., Jones, R. A., The acoustical impedance presented by some human ears to hearing-aid earphones of the insert type. Acustica **6** [1956], 339–345.
[24] Joswig, M., Messung der Trommelfellimpedanz des Menschen mit der Meßrohrmethode. Fortschritte der Akustik – DAGA 1981, DPG-Verlag, Bad Honnef 1981, 709–712.
[25] Hung, I. J., Dallos, P., Study of the acoustic reflex in human beings I. Dynamic characteristics. J. Acoust. Soc. Amer. **52** [1972], 1168–1180.
[26] Lutman, M. E., Martin, A. M., Development of an electroacoustic analogue model of the middle ear and acoustic reflex. J. Sound Vib. **64** [1979], 133–157.
[27] Rabinowitz, W. M., Acoustic-reflex effects on the input admittance and transfer characteristics of the human middle ear, Ph.D. Thesis, MIT, Cambridge MA 1977.
[28] Møller, A. R., Acoustic reflex in man. J. Acoust. Soc. Amer. **34** [1962], 1524–1534.